

# Solar Oscillation Frequency Changes on Time Scales of Nine Days

S. C. Tripathy<sup>1</sup> · F. Hill<sup>1</sup> · K. Jain<sup>1</sup> ·  
J. W. Leibacher<sup>1,2,3</sup>

Received: date / Accepted: date

© Springer Science+Business Media B.V. ....

**Abstract** We establish that global solar  $p$ -mode frequencies can be measured with sufficient precision on time scales as short as nine days to detect activity-related shifts. Using ten years of GONG data, we report that mode-mass and error-weighted frequency shifts derived from nine days are significantly correlated with the strength of solar activity and are consistent with long-duration measurements from GONG and the SOHO/MDI instrument. The analysis of the year-wise distribution of the frequency shifts with change in activity indices shows that both the linear-regression slopes and the magnitude of the correlation varies from year to year and they are well correlated with each other. The study also indicates that the magnetic indices behave differently in the rising and falling phases of the activity cycle. For the short-duration nine-day observations, we report a higher sensitivity to activity.

**Keywords:** Sun: activity, Sun: oscillations, Sun: helioseismology

## 1 Introduction

It is now well established that the global oscillation frequencies of the Sun change in phase with the solar activity cycle, see for example Jain and Bhatnagar (2003) for intermediate-degree modes, Jiménez-Reyes *et al.* (2004) and Howe *et al.* (2006) for low-degree modes, and references therein. However, there is still no consensus regarding the physical mechanism that gives rise to these changes (Kuhn, 2001). One deficiency is the lack of measurements for modes at high frequency and high degree (Rhodes, Reiter, and Schou, 2003) and little information about the correlation on short time scales. Since the  $p$ -mode frequency changes are thought to be associated with individual active regions that come and go continuously (Hindman *et al.*, 2000), one would anticipate that the frequencies also change continuously on any time scale. Due to the finite lifetime of the modes, the correlation between frequency and activity

---

<sup>1</sup>GONG Program, National Solar Observatory, 950 N. Cherry Avenue, Tucson, AZ 85719, USA  
email: stripathy@nso.edu

<sup>2</sup> Institut d'Astrophysique Spatiale (CNRS), Université Paris-Sud 11, Orsay, France

<sup>3</sup> Observatoire de Paris, LESIA (CNRS), F-92195 Meudon Principal Cedex, France

may depend on the length of the observing run. Thus, the use of mode frequencies and other parameters derived from short time series, during which the solar activity varies less, may help understand the underlying mechanism of these variations.

Rhodes, Reiter, and Schou (2003) used a few sets of three-day time series in the computation and fitting of intermediate-degree  $p$ -mode frequencies and widths. The analysis, using Michelson Doppler Imager (MDI) and Mount Wilson Observatory (MWO) data, resulted in a higher sensitivity as measured from the slope of the linear regression between the frequency shifts and activity differences, compared to the slopes from longer time series. However, the result was not confirmed when Global Oscillation Network Group (GONG) data were used (Rose *et al.*, 2003).

In the domain of low-degree modes, Chaplin *et al.* (2001) studied global modes on different time scales, the shortest of which was 27 days. Their results suggest that the sensitivity to changes in the Kitt Peak magnetic field measurements may be higher in the rising phase of the cycle. Salabert *et al.* (2002) studied high-frequency modes ( $\nu > 3.7$  mHz) with a time series of eight days using IRIS<sup>++</sup> data and confirmed that the frequency shift becomes negative above 4.5 mHz up to the cutoff frequency of 5.5 mHz. A similar trend for intermediate-degree frequencies was reported earlier by Ronan, Cadora, and LaBonte (1994) and Jefferies (1998).

Here, we study short temporal variations in the frequency shifts and their degree of correlation with solar activity over a complete solar cycle. To do so, we use GONG data for the period 1995–2005, which covers partially the descending phase of the cycle 22 and the ascending and descending part of the current solar cycle 23. The analysis is carried out by calculating  $p$ -mode frequencies on a time scale as short as nine days.

## 2 Data

### 2.1 Extraction of Mode Frequencies

We examine time series of nine-days length which were processed with a multi-taper spectral analysis (Komm *et al.*, 1999) to produce power spectra for each spherical harmonic degree ( $\ell$ ) and order ( $m$ ) up to  $\ell = 100$ . The mode frequencies characterized by  $n$ ,  $\ell$ , and  $m$  were estimated by fitting the individual peaks (Anderson, Duvall, and Jefferies, 1990). Each  $(n, \ell)$  multiplet was then fitted to a Legendre polynomial series

$$\nu_{n\ell m} = \nu_{n\ell} + \sum_{j=1}^{j_{\max}} a_j(n, \ell) P_j(m/\ell), \quad (1)$$

to find the central frequency ( $\nu_{n\ell}$ ) of the multiplet. Here,  $P_j$  is the Legendre polynomial of order  $j$ ,  $a_j$  are the splitting coefficients, and we take  $j_{\max}$  to be nine. Since the optimal number of tapers depends on the length of the time series (Komm *et al.*, 1999), we use three generalized-sine tapers for the nine-day time series as opposed to five for the standard GONG procedure which measures frequencies from time series of 108 days duration. It should be noted that not all modes are fitted successfully at every epoch due to the stochastic nature of the modes. More details of the procedure can be found in Hill *et al.* (1996).

The GONG data analyzed here consist of 424 nine-day time intervals and cover a period of more than ten years between 7 May 1995 and 16 October 2005. Each

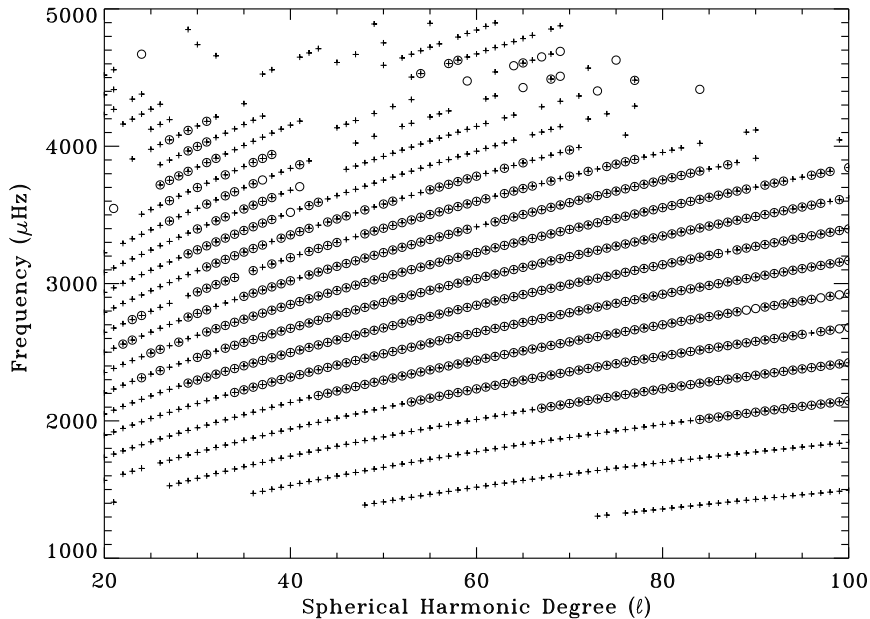


**Figure 1** The  $\ell - \nu$  diagram showing oscillation modes for  $\ell \geq 20$ . The circles denote the modes obtained from nine-day sample covering the period 16–24 September 2004 while the pluses represent the modes from 108-day sample corresponding to the period 8 August to 21 October 2004.

individual nine-day set yields about 650  $(n, \ell)$  multiplets in the degree range of  $20 \leq \ell \leq 100$ . In Figure 1, we compare mode frequencies as a function of  $\ell$  obtained from one sample of nine-day and 108-day (standard GONG product<sup>1</sup>) time series. It is evident that fewer modes are fitted from the nine-day power spectra, particularly at low and high frequencies. Differences between the modes that are present in both data sets are not visible on this scale. Further, we notice a few modes in the nine-day sample that are not present in the 108-day sample, probably due to their short lifetime.

## 2.2 Activity Indices

We have studied the correlation of the frequencies with five well-known surface activity indicators observed over the visible surface of the Sun. These are: the integrated radio flux at 10.7 cm ( $F_{10}$ ) obtained from Solar Geophysical Data<sup>2</sup> (SGD), the core-to-wing ratio of the Mg II line at 2800 Å (Mg II)<sup>3</sup>, the Mt. Wilson magnetic plage strength index (MPSI) and the Mt. Wilson sunspot index (MWSI) from Mount

<sup>1</sup><http://gong.nso.edu/data>

<sup>2</sup><http://www.ngdc.noaa.gov/stp/stp.html>

<sup>3</sup><http://www.sec.noaa.gov/ftpdir/sbuV/NOAAMgII.dat>

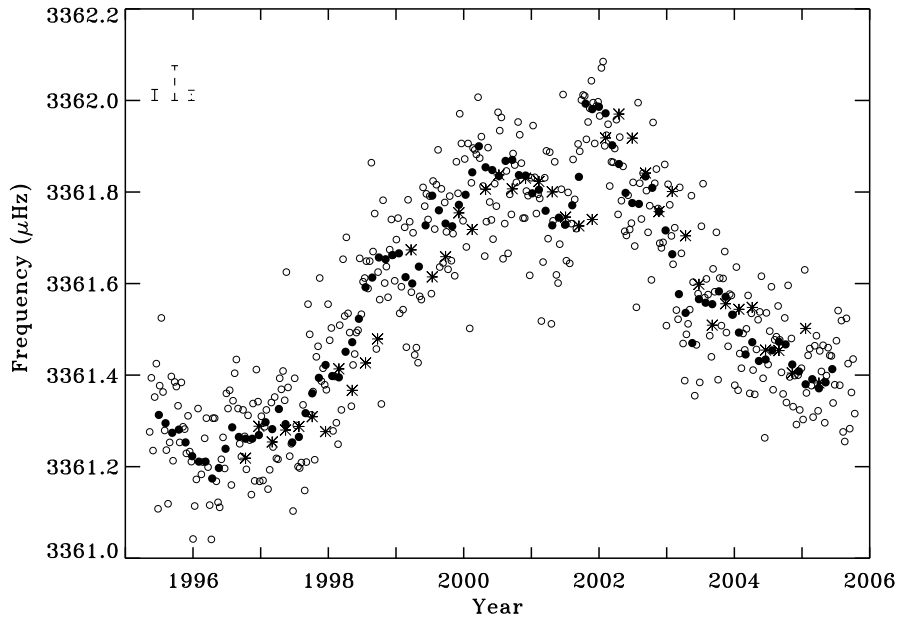


**Figure 2** Variation of the central frequency for the  $n = 9$ ,  $\ell = 81$  mode. The open and filled circles represent nine and 108-day time samples from GONG respectively while the stars represent the 72-day MDI data. The lines on the upper-left-hand corner shows representative uncertainties in fitting corresponding to GONG (dashed line for nine days and solid line for 108 days) and MDI (dotted) frequencies respectively.

Wilson magnetograms (Ulrich, 1991), and the International Sunspot number ( $R_I$ ) obtained from SGD. These different measures of solar activity probe the solar atmosphere at different levels and show different degrees of correlation with oscillation frequencies (Bachmann and Brown, 1993; Bhatnagar, Jain, and Tripathy, 1999).

### 3 Analysis

As a specific example of the temporal variation of frequency, we show a single mode corresponding to the  $n = 9$ ,  $\ell = 81$  multiplet as a function of time in Figure 2. We also include the same mode from MDI data for corroboration. A distinct temporal variation can be seen in all of the data sets. The change over the solar cycle is about  $1 \mu\text{Hz}$  for the nine-day frequencies which is approximately 12 times larger than the formal uncertainty of  $0.075 \mu\text{Hz}$  in the frequency determination. The change in the 108-day GONG frequencies and 72-day MDI frequencies appears to be a smooth average of the nine-day frequencies.

There are different definitions for calculating frequency shifts (Howe, Komm, and Hill, 2002). Here we follow the approach of Woodard *et al.* (1991) and define the mean

frequency shift ( $\delta\nu$ ) as the mode-inertia weighted sum of the measured frequencies:

$$\delta\nu(t) = \sum_{n,\ell} \frac{Q_{n\ell}}{\sigma_{n,\ell}^2} \delta\nu_{n,\ell}(t) / \sum_{n,\ell} \frac{Q_{n,\ell}}{\sigma_{n,\ell}^2}, \quad (2)$$

where  $\sigma_{n,\ell}$  is the uncertainty in the frequency measurement,  $\delta\nu_{n,\ell}(t)$  is the change in a given multiplet of  $n$  and  $\ell$ , and  $Q_{n,\ell}$  is the inertia ratio as defined by Christensen-Dalsgaard and Berthomieu (1991). The reference frequency is chosen in such a way that it corresponds to a minimum value of the activity; the 36th set covering the period 17–25 March 1996 was used.

In order to investigate the variation of the frequencies with solar activity, we correlate and fit the shifts against the activity differences using the expression

$$\delta\nu = a \delta I + b \quad (3)$$

to give the best linear fit to the data. The slope ( $a$ ) which measures the shift per activity index and hence sensitivity of the shift, and the intercept ( $b$ ) are obtained from the linear least-square fit for each of the activity index ( $I$ ). Following the definition of frequency shift,  $\delta I$  is calculated by taking the 36th data point as the reference activity unless mentioned otherwise in the text.

## 4 Results and Discussions

Figure 3 shows the mean frequency shifts as a function of the epoch (left panel) and the change in activity (right panel) for two activity indices; one magnetic (MPSI) and the other non-magnetic ( $F_{10}$ ). It is reassuring to see that the mean frequency shifts derived from nine-days clearly show a similar solar cycle variation to those derived from longer time series. The only difference is the rapid fluctuations seen in each of the plots which arises due to the short interval over which the mean frequency shifts and mean activity differences are calculated. The solid lines in the two right-hand panels represent the straight lines obtained by using Equation (3) to give the best linear fits to the two sets of data points; the corresponding slopes and intercepts of both fits are tabulated in the last rows of Tables 1 and 2. A significant correlation between the frequency shifts and change in activity indices is evident except near the activity-minimum phase of the cycle around 1996–97 reflecting deviations from the assumed linear dependence. We examine this more critically in the next Section.

### 4.1 Year-wise Variations

In order to study how closely the frequencies follow the activity levels, we study year-wise variations. The distribution of the number of points in each year can be seen in Table 1. As before, the mean frequency shift for each year (also for the entire data set) is calculated using Equation (2) but the reference frequency is now considered to be the middle point in each set. Similarly, the middle point in each activity set was considered as the reference activity for the linear regression analysis. For example, for the year 1995, the reference point for calculating the frequency shift and change in activity was taken as the 14th point. The results of the linear least-square fits and correlation coefficients for  $F_{10}$  are summarized in Table 1. For comparison, we

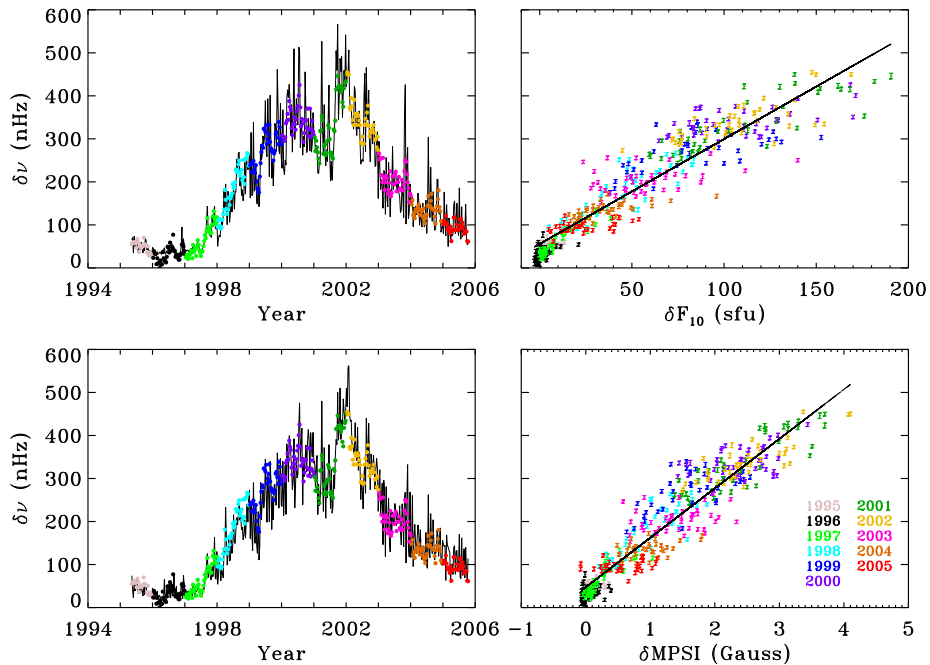


**Figure 3** Mean-frequency shifts plotted as a function of both time (left panels) and change in activity (right panels). The solid lines in the left-hand panels are the scaled frequency differences which result from the two least-squares fits which are shown in the right-hand panels. The solid lines in those two panels denote the linear fits to the frequency differences when regressed upon changes in the 10.7-cm radio flux and upon changes in MPSI. The corresponding slopes and intercepts are given in the last rows of Tables 1 and 2. For clarity, the  $1\sigma$  uncertainties in the mean frequencies are omitted from the left panels. These are visible in the right panels.

also tabulate the slope and correlation coefficient obtained from the entire data set in the last row of the Table 1. We find significant year-to-year variation in the calculated slopes and the correlation coefficients. For a more detailed investigation of the variation in the slopes, we show mean-frequency shifts as a function of the activity differences ( $\delta F_{10}$ ) for four representative years in Figure 4. The solid lines in the four panels represent the linear fits to the pairs of frequency differences and 10.7-cm flux differences in the four different years, while the dashed line which is repeated in all four panels, is the linear fit to all 424 datasets. This linear fit can be considered as the representative fit for the current solar cycle. It is interesting to note that the solid and dashed lines for the year 1997 have similar orientation implying close agreement in the values of the slopes indicating similar mean shifts per unit activity. Surprisingly, the best correlation between the frequency shifts and 10.7 cm radio flux also exists during 1997 which represents the beginning of the rising phase of the current solar cycle. Results for MPSI obtained with the similar analysis are given in Table 2 and Figure 5. For MPSI, a significant correlation is obtained for 1997, 1998, and 2001 and a poor correlation for 1996, 2003, and 2005, and it closely agrees with  $F_{10}$ . Similar results are found for all other activity indices

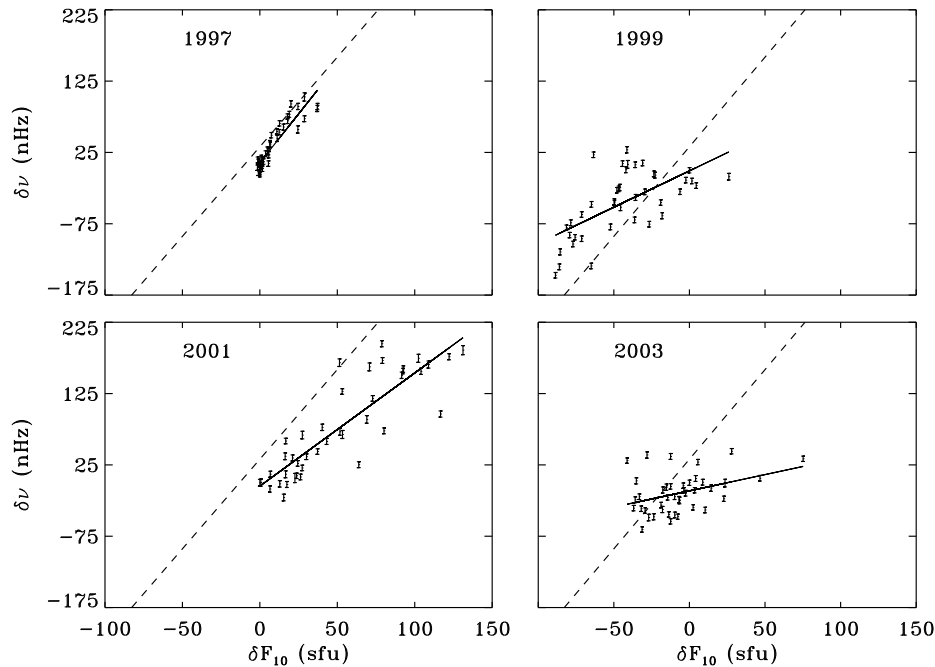


**Figure 4** Mean-frequency shifts plotted as a function of  $\delta F_{10}$  for four selected years as marked on each figure. The solid line denotes the linear fit to the activity measurements for that year. The error bars signify the  $1\sigma$  uncertainties in the mean-frequencies. The dashed line denotes the linear fit to all 424 data points.

considered in this paper. Specifically, we note that the correlation coefficients and slopes obtained from the analysis of the entire data sets are similar to those of 1997 or slightly higher and do not represent average values of the year-wise variations. This can be more clearly visualized in Figure 6 where we have shown the linear fits between the frequency shifts and activity differences using the slopes and intercepts given in Tables 1 and 2. Numerically, the average slopes of the yearly regression fits are 1.26 nHz/sfu for  $F_{10}$  and 52.57 nHz/Gauss for MPSI. These mean slopes are each approximately a factor of two smaller than are the slopes of the overall fits to the corresponding collection of 424 datasets.

In a similar analysis, Woodard *et al.* (1991) have studied the variation of oscillation frequencies during 1986, 1988, and 1989. They report different correlation coefficients for annual variations (except for the magnetic field during 1988 and 1989) which are also different when all the data were taken together. Our result qualitatively agrees with these findings although there are differences in detail. However, the discrepancy can not be investigated further since the two studies do not have common activity indices.

Since the linear regression analysis clearly shows the yearly variations in the slopes and the correlation coefficients, we investigate a possible correlation between these two quantities. This is carried out by plotting the annual variation of the correlation coefficients along with the slopes for four out of the five activity indicators considered

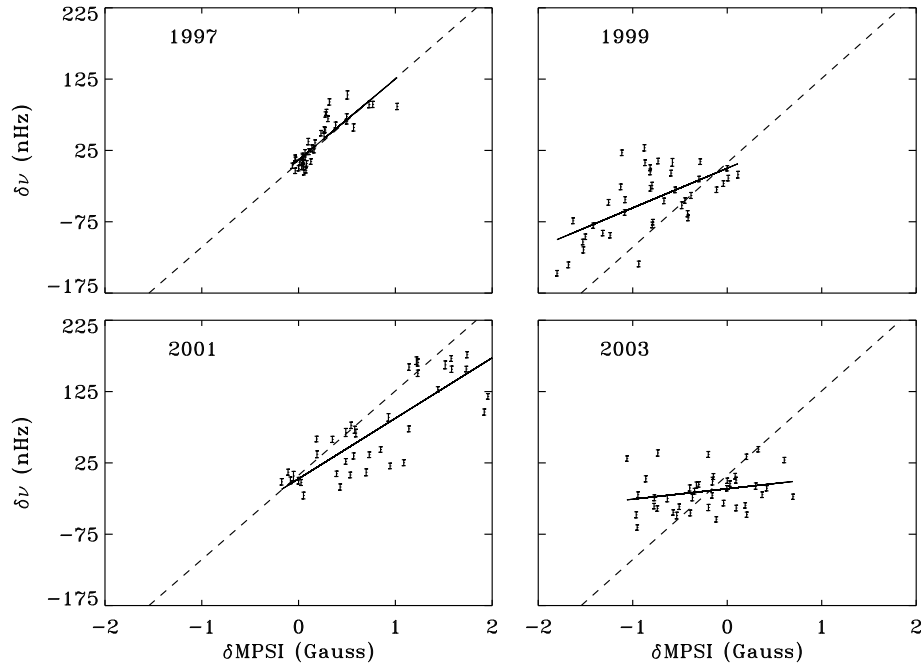


**Figure 5** Same as Figure 4 but for  $\delta\text{MPSI}$

in this paper (Figure 7). The similarity between the two curves stands out in each case signifying strong correlations, although some differences can be seen in detail. The correlation is further confirmed by calculating the linear and rank correlation coefficients between the two quantities (Table 3). The maximum correlation is obtained for Mg II, followed by MPSI while MWSI has the lowest correlation coefficient.

The relationship between the annual linear-regression slopes and yearly averaged solar activity is shown in Figure 8. The striking feature is the strong temporal variability of the regression slopes which do not appear to be correlated with activity indices on the time scale of the solar cycle. On closer examination, there appears to be a good correlation between 1995–1998 and 2001–2005. This could indicate that there are two components of the activity which contribute to the variability of the slopes. The major contribution comes from the overall weak magnetic field, and hence during the ascending and descending phase of the cycle we have a strong correlation with activity. But during the maximum phase of the cycle, when the field is dominated by the strong field, due to the increase in the number and strength of the active regions, the slopes do not follow the activity measurements.



**Table 1** Year-wise distribution of correlation statistics between frequency shifts ( $\delta\nu$ ) and  $\delta F_{10}$ . Shown are the number of data sets ( $N$ ), epoch covered, the mean shift per unit change in activity ( $a$ ) in nHz/sfu, the intercept ( $b$ ) in nHz, Pearson's linear coefficient ( $P_p$ ) Spearman rank correlation coefficient ( $r_s$ ) and its two-sided significance ( $P_s$ ). The last row denotes the values corresponding to all 424 data sets.

$N$	Epoch	$a$	$b$	$P_p$	$r_s$	$P_s$
27	7 May 1995 – 4 January 1996	$1.25 \pm 0.56$	$-6.33 \pm 2.70$	0.40	0.40	$3.9 \times 10^{-2}$
41	5 January 1996 – 7 January 1997	$1.56 \pm 0.53$	$3.42 \pm 3.45$	0.42	0.42	$5.9 \times 10^{-3}$
40	8 January 1997 – 2 January 1998	$2.73 \pm 0.19$	$10.62 \pm 2.68$	0.92	0.92	$6.1 \times 10^{-17}$
41	3 January 1998 – 6 January 1999	$2.14 \pm 0.23$	$5.88 \pm 5.06$	0.83	0.79	$1.1 \times 10^{-9}$
40	7 January 1999 – 1 January 2000	$1.02 \pm 0.20$	$-0.83 \pm 10.40$	0.64	0.64	$9.4 \times 10^{-6}$
41	2 January 2000 – 4 January 2001	$0.69 \pm 0.15$	$-43.47 \pm 4.17$	0.58	0.50	$9.8 \times 10^{-4}$
41	5 January 2001 – 8 January 2002	$1.59 \pm 0.15$	$-4.74 \pm 9.30$	0.87	0.88	$6.4 \times 10^{-14}$
40	9 January 2002 – 3 January 2003	$1.22 \pm 0.18$	$-4.32 \pm 7.09$	0.75	0.76	$1.5 \times 10^{-8}$
41	4 January 2003 – 7 January 2004	$0.46 \pm 0.17$	$-11.38 \pm 4.21$	0.39	0.37	$1.9 \times 10^{-2}$
40	8 January 2004 – 1 January 2005	$0.70 \pm 0.15$	$-3.75 \pm 3.80$	0.60	0.66	$3.4 \times 10^{-6}$
32	2 January 2005 – 16 October 2005	$0.48 \pm 0.18$	$1.13 \pm 2.79$	0.43	0.33	$6.5 \times 10^{-2}$
424	7 May 1995 – 16 October 2005	$2.51 \pm 0.04$	$32.98 \pm 5.54$	0.94	0.95	0.0

**Table 2** Year-wise distribution of correlation statistics between frequency shifts ( $\delta\nu$ ) and  $\delta\text{MPSI}$ . The notations have the same meaning as in Table 1. The units of  $a$  are nHz/Gauss.

$N$	Epoch	$a$	$b$	$P_p$	$r_s$	$P_s$
27	7 May 1995 – 4 January 1996	$51.45 \pm 24.30$	$-4.65 \pm 2.53$	0.39	0.36	$6.2 \times 10^{-2}$
41	5 January 1996 – 7 January 1997	$34.71 \pm 20.30$	$1.49 \pm 4.15$	0.26	0.24	$1.3 \times 10^{-1}$
40	8 January 1997 – 2 January 1998	$113.35 \pm 11.31$	$11.79 \pm 3.64$	0.85	0.87	$2.1 \times 10^{-13}$
41	3 January 1998 – 6 January 1999	$104.59 \pm 11.56$	$40.20 \pm 7.09$	0.82	0.80	$3.4 \times 10^{-10}$
40	7 January 1999 – 1 January 2000	$55.57 \pm 11.51$	$0.06 \pm 11.04$	0.61	0.54	$3.5 \times 10^{-4}$
41	2 January 2000 – 4 January 2001	$28.10 \pm 10.05$	$-48.39 \pm 5.16$	0.41	0.32	$4.0 \times 10^{-2}$
41	5 January 2001 – 8 January 2002	$84.78 \pm 8.04$	$2.79 \pm 8.96$	0.86	0.86	$5.3 \times 10^{-13}$
40	9 January 2002 – 3 January 2003	$61.10 \pm 6.88$	$-5.32 \pm 5.86$	0.82	0.78	$2.3 \times 10^{-9}$
41	4 January 2003 – 7 January 2004	$14.63 \pm 9.39$	$-11.23 \pm 4.77$	0.24	0.27	$8.9 \times 10^{-2}$
40	8 January 2004 – 1 January 2005	$24.29 \pm 8.52$	$-0.06 \pm 4.47$	0.42	0.36	$2.4 \times 10^{-2}$
32	2 January 2005 – 16 October 2005	$5.68 \pm 8.46$	$3.65 \pm 3.10$	0.12	0.11	$5.5 \times 10^{-1}$
424	7 May 1995 – 16 October 2005	$118.25 \pm 2.10$	$7.70 \pm 5.03$	0.94	0.94	0.0

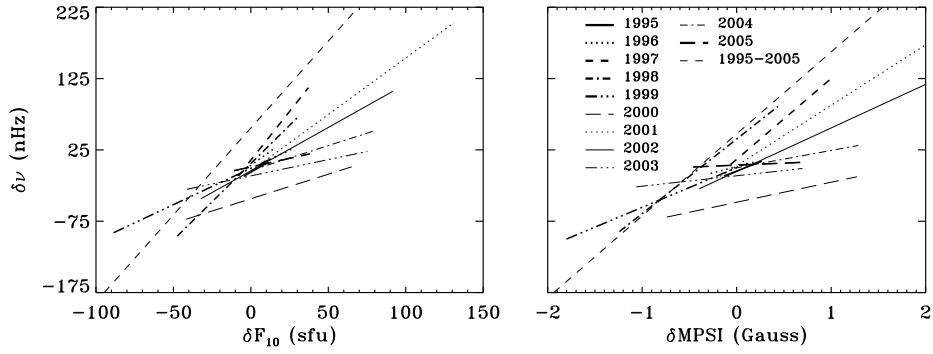


**Figure 6** The panels shows the linear fit between the year-wise frequency shifts and activity differences and are constructed using the slopes and intercept values given in Table 1 (left panel) and Table 2 (right panel).

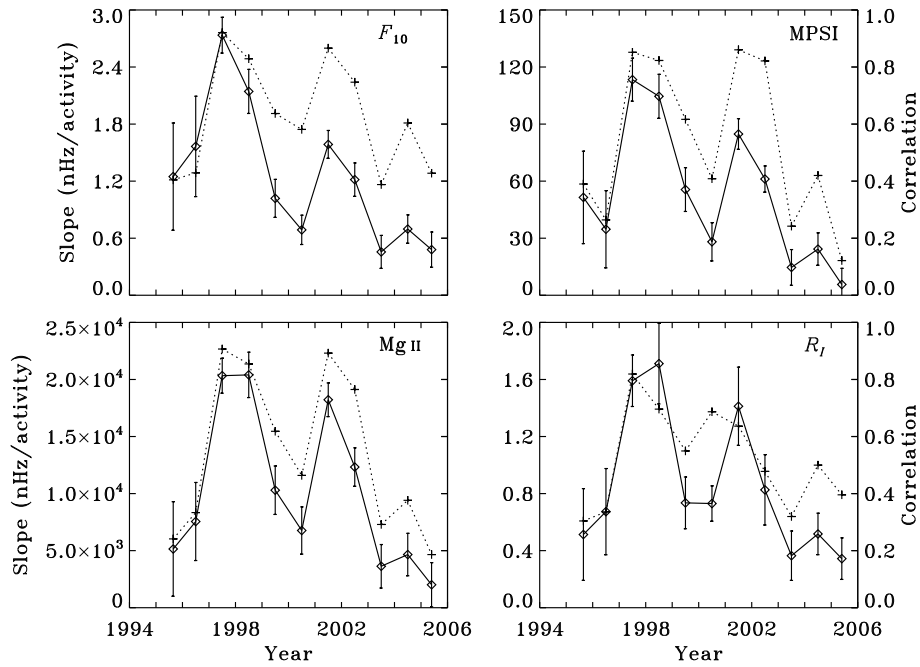


**Figure 7** Year-wise variation of the linear-regression slope (diamonds) and the Pearson's correlation coefficients (pluses) for different activity indices. A strong correlation between the two is clearly visible. The error bars signify the  $1\sigma$  errors in the determination of the slopes.

**Table 3** The correlation statistics between slopes and correlation coefficients for different activity indicators. Shown are the Pearson’s linear coefficient ( $P_p$ ), the rank correlation ( $r_s$ ), and the two-sided significance ( $P_s$ ).

Activity	$P_p$	$r_s$	$P_s$
$F_{10}$	0.72	0.72	$1.1 \times 10^{-2}$
MPSI	0.90	0.89	$2.3 \times 10^{-4}$
MWSI	0.57	0.58	$6.0 \times 10^{-2}$
Mg II	0.96	0.91	$1.1 \times 10^{-4}$
$R_I$	0.81	0.81	$2.6 \times 10^{-3}$

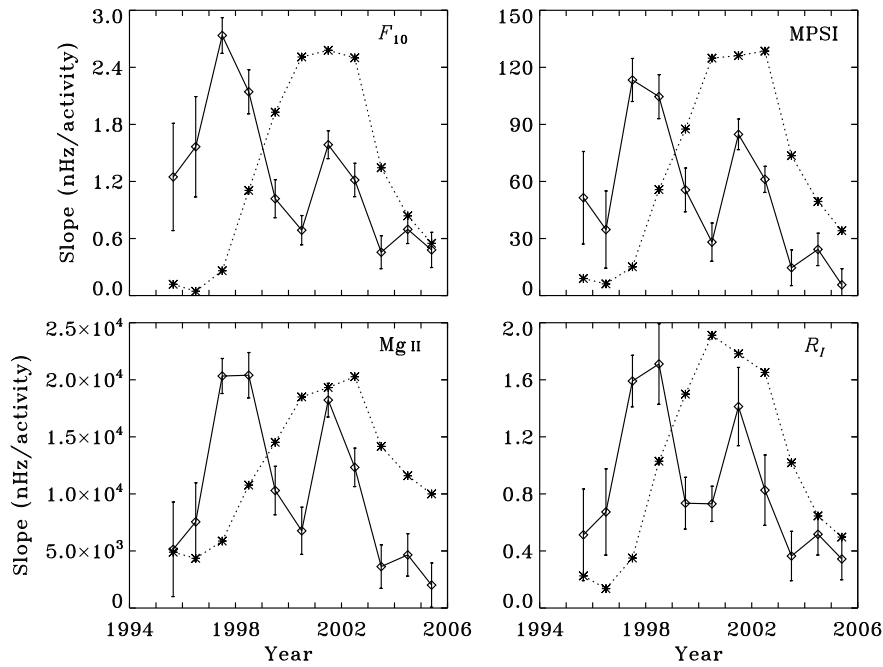


**Figure 8** Temporal dependence of the linear-regression slopes (diamonds) and corresponding yearly-averaged solar activity (stars). The error bars signify the  $1\sigma$  errors in the determination of the slopes.

We finally note that the year-wise variation of the oscillation frequencies is distinctly different than the analysis involving the entire data sets emphasizing that both the long and short-term variations are different in nature. We also find that the long-term variation is not a simple average of the short-term variations. Therefore, we conclude that studies of changes of oscillation frequencies which consider all the data sets together may not accurately represent the variations on a scale which is smaller than the length of the entire data sets.

## 4.2 Variation in Rising and Falling Phases of Activity Cycle 23

From the discussion given in Section 4.1, it is evident that there is no significant difference in the correlation pattern between the magnetic (Table 2) and non-magnetic (Table 1) activity indices. But the analysis of Chaplin *et al.* (2001) involving low-degree modes suggested that the sensitivity to changes in the disk-averaged line-of-sight magnetic field component may be higher during the rising phase of the cycle. We perform a similar analysis by separating our data set into rising and falling phases of activity cycle 23. Since May 1996 and April 2000 mark the minimum and maximum of cycle 23 (see SGD), we choose the period 1 May 1996 – 15 May 2000 consisting of 1476 days as the rising phase. Avoiding the secondary maximum of this cycle, we choose 02 October 2001 – 16 October 2005 again consisting of 1476 days as the falling phase so that both halves have a similar minimum to maximum range in activity indices. Further, to be consistent with the analysis of annual variations,  $\delta I$  is calculated by taking the middle data point in each set as the reference. The results are summarized in Table 4 where we have shown the slopes, the rank correlation coefficients, and the differences in the slopes between descending and ascending phases normalized by their combined uncertainty ( $\sigma_{\delta a}$ ); a negative  $\sigma_{\delta a}$  indicating a higher value for the rising phase. The differences for magnetic indices, MPSI and MWSI, with  $\sigma_{\delta a} > 4$  suggest significant differences in behaviour of the magnetic flux emerging over the ascending and descending phases. The value of 2.79 for the 10.7 cm radio flux implies behaviour similar to the magnetic indices but not as significant as the magnetic flux, while MgII with a value closer to zero implies no phase dependence. The sunspot number, the only index with a positive  $\sigma_{\delta a}$  exhibits an opposite behaviour compared to other indices, but since its value is less than 2, the difference can not be considered to be of significance. This result broadly agrees with the findings of Chaplin *et al.* (2001) where a phase-dependent behaviour for the Kitt Peak magnetic index was reported; but it is not clear why other magnetic indices *e.g.* MPSI and MWSI did not show a similar difference. Our results, on the other hand, shows phase-dependent behaviour for all of the magnetic indices and suggest that the frequency shifts are caused by the magnetic fields at or very near the solar surface.

Similarly, the rank correlations obtained between the frequency shifts and activity indicators also manifest a phase-dependent pattern. In general, the rank correlation coefficients are lower in the descending phase of the activity cycle. The maximum change is seen in the case of MWSI but we should point out that there are significant gaps in the measurement of MWSI index which may contribute to this discrepancy. Finally, we speculate that this phase-dependent behaviour of the frequency shifts with magnetic flux gives rise to the hysteresis pattern seen only in case of the magnetic activity indices (Jiménez-Reyes *et al.*, 1998 and Tripathy *et al.*, 2001).

**Table 4** Results of linear fits to the change in activity indices in the rising and falling phases of cycle 23. Each phase consists of about four years of data. Shown are the mean shift per unit change in activity ( $a$ ), the intercept ( $b$ ), Spearman rank correlation coefficient ( $r_s$ ). The last column ( $\sigma_{\delta a}$ ) gives the difference in the slopes between ascending and descending phases normalized by the combined uncertainty. We have omitted the two-sided significance as these are all zeros indicating high significance except for MWSI with a value of  $10^{-22}$  in the descending phase.

Activity index	Ascending phase			$r_s$	Descending phase			$r_s$	$\sigma_{\delta a}$
	$a$ (nHz/index)	$b$ (nHz)			$a$ (nHz/index)	$b$ (nHz)			
$F_{10}$	$2.54 \pm 0.08$	$180.07 \pm 3.12$	0.95	$2.32 \pm 0.08$	$174.44 \pm 3.66$	0.90	-2.79		
MPSI	$129.72 \pm 3.67$	$142.63 \pm 3.01$	0.94	$109.08 \pm 3.54$	$202.59 \pm 3.28$	0.88	-5.72		
MWSI	$358.29 \pm 26.12$	$167.21 \pm 5.93$	0.86	$248.41 \pm 24.48$	$184.73 \pm 7.23$	0.67	-4.34		
Mg II	$21476 \pm 516$	$162.86 \pm 2.55$	0.95	$21326 \pm 638$	$199.47 \pm 3.07$	0.90	-0.26		
$R_I$	$2.30 \pm 0.08$	$190.29 \pm 3.82$	0.92	$2.49 \pm 0.12$	$184.51 \pm 4.64$	0.84	1.84		

**Table 5** Results of linear fits to differences in activity indices and correlation statistics for frequency shifts obtained from time series of different length. Shown are the length of the time ( $t$ ), the mean shift per unit change in activity ( $a$ ), the intercept ( $b$ ), Pearson’s linear coefficient ( $P_p$ ), Spearman rank correlation ( $r_s$ ). The two-sided significance ( $P_s$ ) is smaller than  $10^{-17}$  and is not shown.

Activity index	$t$ (days)	$a$ (nHz/index)	$b$ (nHz)	$P_p$	$r_s$
$F_{10}$	9	$2.44 \pm 0.04$	$55.72 \pm 3.24$	0.94	0.95
	72	$1.75 \pm 0.04$	$15.37 \pm 2.69$	0.99	0.99
	108	$1.77 \pm 0.02$	$14.57 \pm 1.82$	0.99	0.99
MPSI	9	$114.90 \pm 2.05$	$47.41 \pm 3.27$	0.94	0.94
	72	$79.45 \pm 2.23$	$15.49 \pm 3.57$	0.98	0.98
	108	$80.41 \pm 1.34$	$11.93 \pm 2.14$	0.99	0.98
MWSI	9	$427.6 \pm 22.7$	$123.93 \pm 5.63$	0.68	0.80
	72	$481.7 \pm 40.5$	$34.94 \pm 8.96$	0.87	0.89
	108	$504.6 \pm 25.9$	$29.57 \pm 5.65$	0.89	0.91
Mg II	9	$19621 \pm 344$	$23.38 \pm 3.56$	0.94	0.94
	72	$13601 \pm 494$	$0.26 \pm 5.07$	0.97	0.97
	108	$13330 \pm 312$	$1.47 \pm 3.20$	0.97	0.97
$R_1$	9	$2.40 \pm 0.06$	$65.77 \pm 3.96$	0.90	0.92
	72	$1.81 \pm 0.07$	$12.80 \pm 5.21$	0.97	0.95
	108	$1.85 \pm 0.04$	$8.72 \pm 2.97$	0.97	0.97

### 4.3 Comparison With Standard GONG and MDI Data

It is expected that with longer time series, the determination of the frequencies will be more precise as the uncertainty is inversely proportional to the square root of the length of the time series for resolved modes – those with lifetimes less than the length of the time series (Libbrecht, 1992). Additionally, small fluctuations in activity would be averaged out during the longer time period. Thus, it appears that the correlation between the frequency shift and activity will depend on the length of the observing run. The analysis involving low-degree modes (Chaplin *et al.*, 2001) on different time scales, from 216 days to 27 days, confirms that variations in rank correlation are not inconsistent with the change in accuracy expected for different observing intervals. They also report a small rank-correlation coefficient of the order of 0.67 on the time scale of 27 days which is independent of all of the activity indices. If we extrapolate this result to a temporal interval of nine days, we expect to find a very small correlation between the activity indices and frequency shifts.

We compare our results obtained from three different time samples, nine days and 108 days from GONG, and 72 days from MDI in Table 5. The 108-day GONG data covering the period between 7 May 1995 and 16 October 2005 consists of 104 sets

with an overlapping period of 36 days between the two adjacent data sets. The MDI data consists of 46 intervals spanning the period from 1 May 1996 to 16 October 2005. The reference frequency for each data set is chosen in such a way that it corresponds to a minimum value of the activity. From Table 5, we find that all three correlations are highly significant with slight variations in the degree of correlation probably due to the different length of the time series. For the nine-day frequencies, we find the smallest correlation coefficients but they are significantly higher than the values corresponding to analysis of low-degree modes on time scale of 27 days (Chaplin *et al.*, 2001). Since localized active regions have much more power at high degrees, the low and intermediate-degree modes have different responses to activity indices. We also note that for a data set of given length, no significant difference is found between correlations among different activity indices except in the case of MWSI. This is probably due to the large number of gaps in the data which resulted in a poor average when the average was taken over nine days and had no significant effect for averages taken over longer periods.

Similar evidence for different behaviour between low and intermediate-degree modes comes from the comparison of the sensitivity values. We find a higher sensitivity for the short-duration frequencies and confirm the findings of Rhodes, Reiter, and Schou (2003). However, we do not find any explanation for the results of Rose *et al.* (2003) who could not confirm the higher value of sensitivity using GONG<sup>++</sup> data. It is possible that during the high-activity period of 2001, the variation in sensitivity is too small to be detected. This result is again different from that of Chaplin *et al.* (2001), who found similar values for all time intervals considered in their study. Finally, it is worth noting that only in the case of the MWSI index, the slope from the nine-day time series is smaller than the slopes from either the 72- or 108-day time series and may again be attributed to the problem of data gaps as discussed earlier.

#### 4.4 Correlation of Individual Modes

In order to investigate the differences that exist between the low and intermediate-degree modes and between different lengths of the observing run, we carry out the same fitting and correlation analysis for each individual mode using only the GONG data. The Spearman rank correlation coefficients for  $\delta$ MPSI are shown in Figure 9. It is evident that the correlation is a function of frequency and shows a three-part structure: a rise in the low-frequency range, a plateau in the five-minute band, and a decrease in the high-frequency zone. In the case of nine days (top panel of Figure 9), the extent of the plateau region is small indicating that a high value of correlation exists only for a small mode set. On average, it appears that the nine-day correlation coefficients are small compared to the 108-day coefficients confirming that the correlation is a function of the length of the observation. We also note negative coefficients indicating anti-correlation at low ( $\nu < 1700 \mu\text{Hz}$ ) and high ( $\nu > 4200 \mu\text{Hz}$ ) ends of the frequency range. Similar anti-correlation has been reported by Ronan, Cadora, and LaBonte (1994), Harvey (1995), Jefferies (1998), and Rhodes, Reiter, and Schou (2003). However, the frequency range where the shift becomes negative is different in our study than those reported earlier. One possible explanation of the discrepancy could be the lack of sufficient modes at higher frequencies in this analysis. Further work is needed to understand the source of the difference and is beyond the scope of the present paper.



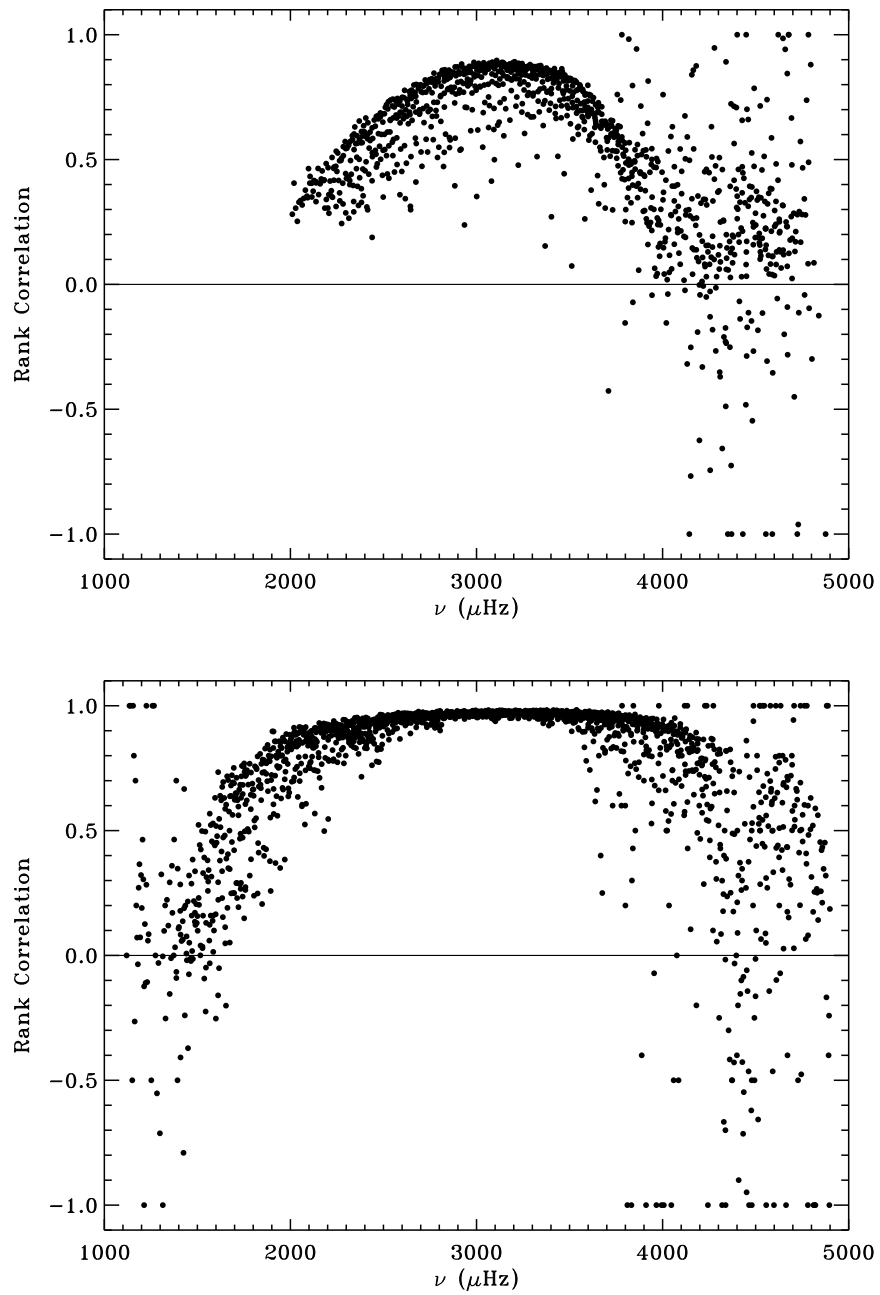


**Figure 9** The Spearman rank correlation coefficients, as a function of frequency, between the weighted frequency shifts and  $\delta\text{MPSI}$  for all modes present in nine-day (top panel) and 108-day frequency determinations (bottom panel).

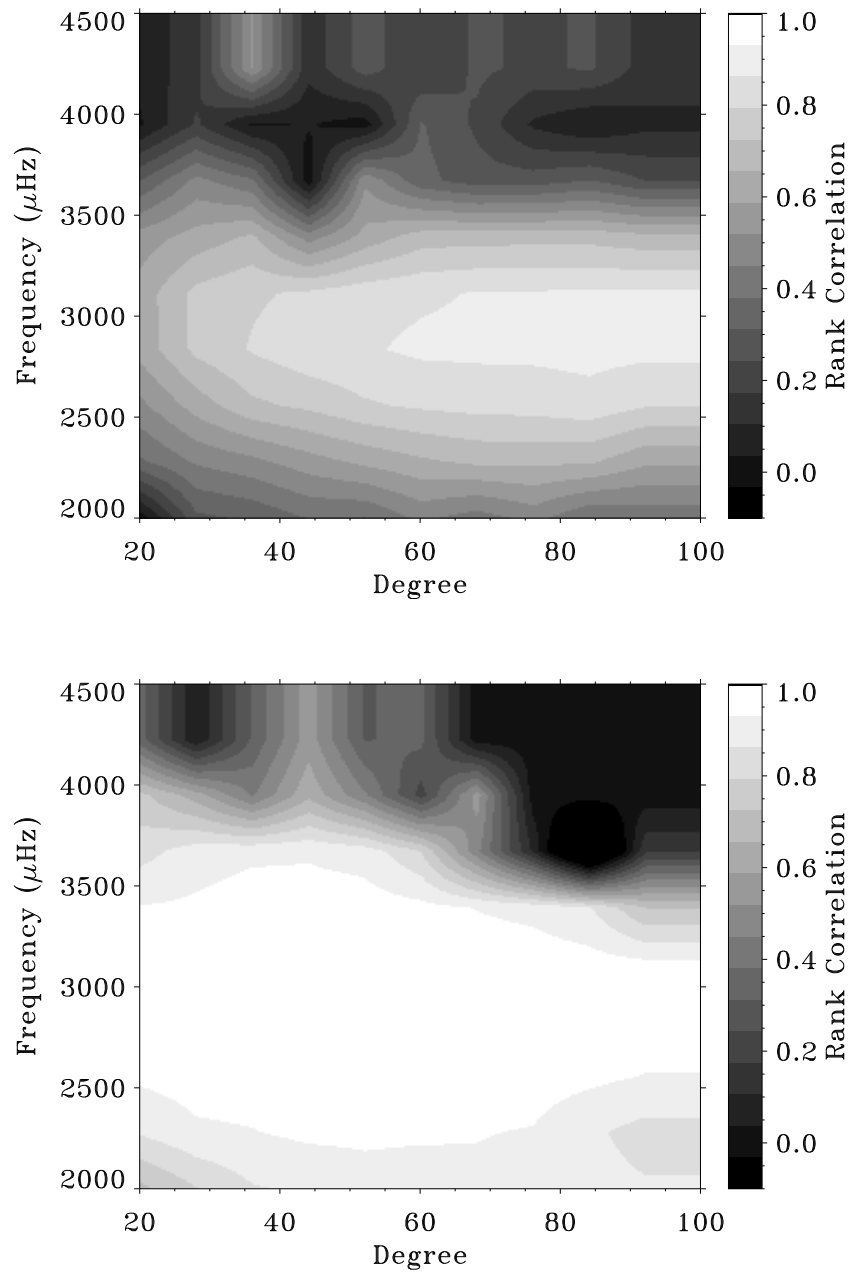


**Figure 10** Correlation maps between the frequency shifts of individual modes and  $\delta\text{MPSI}$  as a function of degree ( $\ell$ ) and frequency ( $\nu$ ). The coefficients obtained from Spearman's rank correlation analysis are binned with a bin size of eight in  $\ell$  and 300  $\mu\text{Hz}$  in  $\nu$ . The top and bottom panels correspond to frequencies measured from nine days and 108 days duration, respectively.

To better illustrate the dependence of the correlation on mode characteristics, we make rank correlation maps as a function of  $\ell$  and  $\nu$  for all modes in nine-day and 108-day data sets with a bin size of eight in  $\ell$  and 300  $\mu\text{Hz}$  in  $\nu$  (Figure 10). In addition to the frequency dependence of the correlation seen in Figure 9, these maps show a decreasing correlation with decreasing  $\ell$  for the nine-day sets. This decrease is markedly smaller for the 108-day analysis. The effect may arise from the increase of the mode lifetime with decreasing  $\ell$ . Longer-lived modes will be observed less often in short time series due to the greater temporal interval between excitation events. The decrease of the signal-to-noise ratio at low frequencies and low degrees may also play a role. Since the value of correlation decreases at low-degree and low frequency, it seems possible that, for low-degree modes ( $\ell \leq 3$ ), it may drop to the values observed by Chaplin *et al.* (2001). Figure 10 emphasizes that the correlation between frequency shifts and activity indices are complex and have different behaviours for different mode sets and observing periods.

## 5 Summary

Using GONG time series over a period of ten years from 7 May 1995 to 16 October 2005, we have computed frequencies for periods of nine days. The high quality data allowed us to study the frequencies of a single mode and we demonstrate that individual multiplets show significant temporal variations with the solar activity cycle. We find that the frequency shifts exhibited by the nine-day time series are consistent with the longer time series used for studies of internal structure measurements and dynamics, and the frequency shift is significantly correlated with different activity indices representing different heights in the solar atmosphere. Further, we show that the correlation between frequency shift and the change in activity indices varies on a yearly basis and is a function of the sensitivity factor as measured from the slope of the linear fits. Although, the slopes do not have a simple relation with the change in activity indicators, the slopes and magnitude of the correlation between the mean frequency shifts and mean activity measures are well correlated. The analysis further demonstrates that there are significant differences between long-term and short-term variations and averages of short-term variations may not accurately reflect the long-term variations and vice-versa.

We also find clear evidence of the phase dependence of the shifts for magnetic activity indices (MWSI and MPSI) showing significant differences in behaviour of the magnetic flux emerging over the ascending and descending phases and confirm the low-degree results of Chaplin *et al.* (2001). Although, there is no significant difference in correlation between frequencies obtained from different observing lengths, the sensitivity factor is higher for frequencies obtained from short-duration time series agreeing with the result of Rhodes, Reiter, and Schou (2003). Finally, from the study of individual modes, we infer that correlation between the shifts and activity indices is complex. More work is needed to understand and find a physical mechanism that could explain the detailed behaviour of the frequency shifts.

**Acknowledgements** We thank the referee for comments which have improved the manuscript substantially. This work was supported by NASA grants NNG 5-11703 and NNG 05HL41I. This work utilizes data obtained by the Global Oscillation Network Group (GONG) program, managed by the National Solar Observatory,

which is operated by AURA, Inc. under a cooperative agreement with the National Science Foundation. The data were acquired by instruments operated by the Big Bear Solar Observatory, High Altitude Observatory, Learmonth Solar Observatory, Udaipur Solar Observatory, Instituto de Astrofísica de Canarias, and Cerro Tololo Interamerican Observatory. This study also includes data from SOHO/MDI. SOHO is a mission of international cooperation between ESA and NASA. This study includes data from the synoptic program at the 150-Foot Solar Tower of the Mt. Wilson Observatory. The Mt. Wilson 150-Foot Solar Tower is operated by UCLA, with funding from NASA, ONR, and NSF, under agreement with the Mt. Wilson Institute. We thank Lawrence Puga for the Mg data.

## References

- Anderson, E.R., Duvall, Jr., T.L., Jefferies, S.M.: 1990, *Astrophys. J.* **364**, 699.
- Bachmann, K.T., Brown, T.M.: 1993, *Astrophys. J.* **411**, L45.
- Bhatnagar, A., Jain, K., Tripathy, S.C.: 1999, *Astrophys. J.* **521**, 885.
- Chaplin, W.J., Elsworth, Y., Issak, G.R., Marchenkov, K.I., Miller, B.A., New, R.: 2001, *Monthly Notices Roy. Astron. Soc.* **322**, 22.
- Christensen-Dalsgaard, J., Berthomieu, J.: 1991, In: Cox, A.N., Livingston, W.C., Matthews, M. (eds.) *Solar Interior and Atmosphere*, Univ. Arizona Press, Tucson, 401.
- Harvey, J.: 1995, In: Hoeksema, J.T., Domingo, V., Fleck, B., Battrick, B. (eds.) *Proc. of Fourth SOHO Workshop: Helioseismology, ESA SP-376*, 9.
- Hill, F. *et al.*: 1996, *Science* **272**, 1292.
- Hindman, B., Haber, D., Toomre, J., Bogart, R.: 2000, *Solar Phys.* **192**, 363.
- Howe, R., Komm, R.W., Hill, F.: 2002, *Astrophys. J.* **580**, 1172.
- Howe, R., Chaplin, W.J., Elsworth, Y., Hill, F., Komm, R.W., Isaak, G.R., New, R.: 2006, *Monthly Notices Roy. Astron. Soc.* **369**, 933.
- Jain, K., Bhatnagar, A.: 2003, *Solar Phys.* **213**, 257.
- Jain, K., Tripathy, S.C., Bhatnagar, A., Kumar, B.: 2000, *Solar Phys.* **192**, 487.
- Jefferies, S.M.: 1998, In: Deubner, F., Christensen-Dalsgaard, J., Kurtz, D. (eds.) *New Eyes to See Inside the Sun and Stars, IAU Symp.* **185**, 415.
- Jiménez-Reyes, S.J., Régulo, C., Pallé, P.L., Roca Cortés, T.: 1998, *Astron. Astrophys.* **329**, 1119.
- Jiménez-Reyes, S.J., García, R.A., Chaplin, W.J., Korzennik, S.G.: 2004, *Astrophys. J.* **610**, L65.
- Komm, R.W., Gu, Y., Hill, F., Stark, P.B., Fodor, I.K.: 1999, *Astrophys. J.* **519**, 407.
- Kuhn, J.R.: 2001, In: Wilson, A. (ed.) *Proc. of SOHO 10/GONG 2000 Workshop: Helio- and Asteroseismology at the Dawn of the Millennium, ESA SP-464*, 7.
- Libbrecht, K.G.: 1992, *Astrophys. J.* **387**, 712.
- Rhodes, E.J., Jr., Reiter, J., Schou, J.: 2003, In: Sawaya-Lacoste, H. (ed.) *Proc. of SOHO 12/GONG+ 2002, Local and Global Helioseismology: the Present and Future, ESA SP-517*, 173.
- Ronan, R.S., Cadora, K., LaBonte, B.J.: 1994, *Solar Phys.* **150**, 389.
- Rose, P., Rhodes, E.J., Jr., Reiter, J., Rudnisky, W.: 2003, In: Sawaya-Lacoste, H. (ed.) *Proc. of SOHO 12/GONG+ 2002, Local and Global Helioseismology: the Present and Future, ESA SP-517*, 373.
- Salabert, D., Jiménez-Reyes, S.J., Fossat, E., Cacciani, A., Ehgamberdiev, S., Gelly, B., Grec, G., Hoeksema, J.T., Khalikov, S., Lazrek, M., Pallé, P., Schmider, F.X., Tomczyk, S.: 2002, In: Sawaya-Lacoste, H. (ed.) *Proc. of the Second Solar Cycle and Space Weather Euroconference, SOLSPA 2001, ESA SP-477*, 253.
- Tripathy, S.C., Kumar, B., Jain, K., Bhatnagar, A.: 2001, *Solar Phys.* **200**, 3.
- Ulrich, R.K.: 1991, *Adv. Space Res.* **11**(4), 217.
- Woodard, M.F., Kuhn, J.R., Murray, N., Libbrecht, K.G.: 1991, *Astrophys. J.* **373**, L81.